

Edge-dependent selection rules in magic triangular graphene flakes

J. Akola, H. P. Heiskanen, and M. Manninen

NanoScience Center, Department of Physics, P.O. Box 35, FI-40014 University of Jyväskylä, Jyväskylä, Finland

(Received 20 March 2008; published 27 May 2008)

The electronic shell and supershell structure of triangular graphene quantum dots has been studied using density functional and tight-binding methods. The density functional calculations demonstrate that the electronic structure close to the Fermi energy is correctly described with a simple tight-binding model, where only the p_z orbitals perpendicular to the graphene layer are included. The results show that (i) both at the bottom and at the top of the p_z band, a supershell structure similar to that of free electrons confined in a triangular cavity is seen, (ii) close to the Fermi level, the shell structure is that of free *massless* particles, (iii) triangles with armchair edges show an additional sequence of levels (“ghost states”) absent for triangles with zigzag edges while the latter exhibit edge states, and (iv) the observed shell structure is rather insensitive to the edge roughness.

DOI: [10.1103/PhysRevB.77.193410](https://doi.org/10.1103/PhysRevB.77.193410)

PACS number(s): 73.21.La, 61.48.De, 81.05.Uw

Recent experimental success in manufacturing single layer graphene flakes on various surfaces^{1–4} has made graphene a new playground for theoretical and computational physics,^{5–9} and more and more experimental results are emerging.^{10–12} Most of the recent interest has been focused in the effects caused by the peculiar band structure of graphite near the Fermi level (ϵ_F): Electrons and holes behave as massless particles (Dirac fermions) due to the linear dispersion relation although their velocity is very small.¹³

The triangular shape of two-dimensional clusters is particularly interesting because, in the case of free electrons, it supports perhaps the most persistent and regular supershell structure of all systems.¹⁴ Furthermore, the triangular shape is preferred in two-dimensional metallic systems^{15,16} and in plasma clusters.¹⁷ For tetravalent elements, triangular clusters have been observed in silicon.¹⁸ It is reasonable to expect that such shapes can be observed also for carbon, and this is supported further by the fact that equilateral triangles of graphene can be cut with the two most stable edge structures, the zigzag edge and the armchair edge.

In this Brief Report, we wish to point out that finite graphene flakes (or quantum dots) have an intriguing energy spectrum close to the Fermi level. We have performed electronic structure calculations for triangular graphene flakes using the density functional theory (DFT) for all the valence electrons and a tight-binding (TB) approach that considers only the carbon p_z electrons (Hückel model). Our results show that already in small triangular flakes ($N=300$, $L=5$ nm), the electronic levels close to ϵ_F can be understood as those of free massless electrons confined in a triangular cavity. Especially, we demonstrate that the edge structure has a selective role in the electronic shell structure: The zigzag edge prohibits a whole sequence of localized states *inside* the cluster although it supports edge states. This leads to well-defined edge-dependent selection rules that are based on an analytical model. Recently, Yamamoto *et al.*¹⁹ addressed the presence (absence) of edge states at ϵ_F in zigzag (armchair) triangles of graphene, and the effect on the optical absorption, but the simple principles of the underlying energy spectrum have remained unexplained.

It is well known that the atomic p_z electrons perpendicular to the graphene plane are responsible for the captivating

band structure shown in Fig. 1 with the valence and the conduction bands meeting at the corners of the hexagonal Brillouin zone.^{20,21} The Fermi surface consists of a discrete set of these points of high- k value, and the resulting density of states (DOS) has a zero weight at ϵ_F . The crossover regions have locally hourglass-like shapes, which results in the linear and isotropic electron dispersion relation in the conduction band ($\epsilon > \epsilon_F=0$) but only in a small energy interval. Since the atomic p_z electrons are perpendicular to the graphene plane, their interaction with the neighboring atoms does not have any directional dependence and, consequently, they can be described as s -type electrons in the TB model. By neglecting also the differential overlap between atomic sites, the system can be described with the traditional Hückel model

$$H_{ij} = \begin{cases} -t, & \text{if } i, j \text{ nearest neighbors} \\ 0, & \text{otherwise} \end{cases},$$

where the hopping parameter t (resonance integral) determines the width of the bands and the on-site energy is chosen to be $\epsilon_F=0$. We choose to present our results in units $t=1$. The resulting TB bands (Fig. 1) reaches from -3 to $+3$ (in real graphene, our unit t corresponds to about 2.6 eV).

A conceptual cutting of a finite graphene flake breaks covalent bonds, yielding edges with dangling bonds. We consider the dangling bonds to be passivated, say, with hydrogen. Since the covalent bonding with hydrogen involves sp^2 hybridized orbitals, the passivation is expected to have only a small effect on the perpendicular p_z electron states. Therefore, we neglect this effect in our TB model and follow Areshkin *et al.*²¹ and treat the edge atoms in the same footing as bulk atoms. Moreover, we will completely neglect the interaction of graphene with the possible substrate and treat the graphene flake as an isolated two-dimensional cluster or quantum dot. As we shall see, the results of the simple TB model agree well with those of the full DFT calculation.

It has been shown that at the bottom of the valence band, the TB model exactly gives the free electron states for a triangular lattice,²² and the same is true also for the hexagonal graphene. Consequently, at the bottom (and at the top),

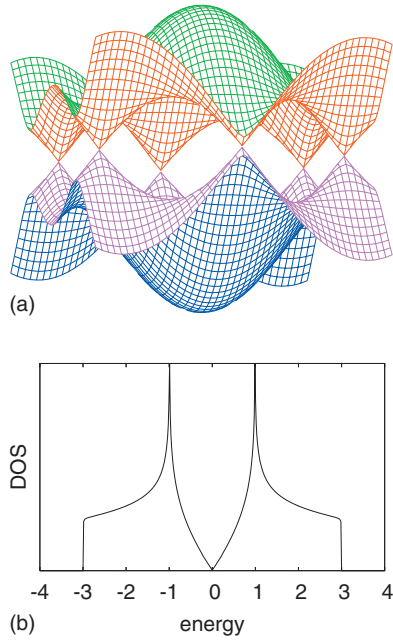


FIG. 1. (Color) Crossover of the valence and conduction bands at the Fermi energy (top) and the density of states (bottom, p_z electrons) of an infinite graphene sheet.

the energy levels are expected to show the same shell structure as free electrons in a triangular cavity, which is determined by the equation^{23,24}

$$\epsilon_{n,m} = \epsilon_0(n^2 + m^2 - nm), \quad (1)$$

where $\epsilon_0 = 8\pi^2\hbar^2/3m_eL^2$, with L being the length of the triangle side. The quantum numbers must satisfy $m \geq 1$ and $n \geq 2m$. Determination of the electron effective mass in the graphene lattice for the TB model gives $\epsilon_0 = 4\pi^2t/9N$, where N is the number of atoms in the triangle ($L = 3d\sqrt{N}/2$ for a large triangle, d is the nearest-neighbor distance).

The shell structure manifests itself as a regular variation of DOS, which can be determined by the Gaussian convolution of the discrete levels. Figure 2 shows DOS close to the bottom of the valence band obtained from the above equation and compared to the TB model for two graphene triangles, one with 10 000 atoms (zigzag edge) and the other with 9918 atoms (armchair edge). The profiles are clearly similar and exhibit the beating pattern of the supershell structure.²⁵ Note that DOS is plotted as a function of $\sqrt{\epsilon+3t}$, making the shells equidistant. Figure 2 shows also the electron densities corresponding to the six lowest energy levels (for degenerate states, we show the sum of the density). The density patterns are identical to those of free electrons confined in a triangle¹⁶ or wave modes in triangular resonators.²⁶

The Fermi level of graphene consists of two equivalent points at the border of the Brillouin zone (see Fig. 1), where the conduction and valence bands open as circular cones, resulting a linear dispersion relation for electrons $\epsilon(\mathbf{k}) = C\hbar k$, where C is the velocity. Thus, it is to be expected that the electron dynamics is not determined by the Schrödinger equation but by the wave equation of massless particles (or the Dirac equation). For free particles confined

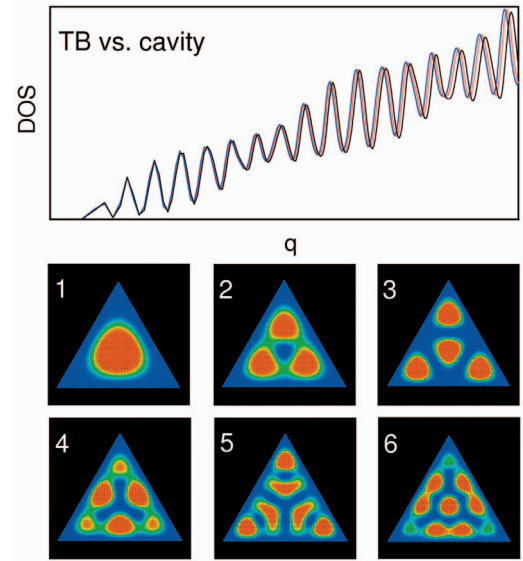


FIG. 2. (Color) Upper panel: DOS at the bottom of the TB band shown as a function of $q = \sqrt{\epsilon+3t}$. Blue: zigzag triangle with 10 000 atoms; red: armchair triangle with 9 918 atoms; and black: result for free electrons in a triangular cavity. Lower panel: Electron densities of the six lowest energy levels.

in a triangle, the energy levels are still determined by Eq. (1), but now it results in the square of the energy, i.e.,

$$\epsilon_{n,m} = \epsilon_1\sqrt{n^2 + m^2 - nm}, \quad (2)$$

where $\epsilon_1 = 2\pi t/\sqrt{3N}$. It is interesting to note that these energy levels were actually computed for the wave equation much earlier than for the Schrödinger equation.²³

Figure 3 shows TB-DOS above the Fermi energy for two large triangles ($\sim 10\,000$ atoms) with zigzag and armchair edges and compares them to the levels of free massless electrons [Eq. (2)]. The results are the following. (i) Each energy level has an additional degeneracy of two due to the two equivalent points at ϵ_F . (ii) The zigzag triangle shows the levels of Eq. (2) with index values $m \geq 1$ and $n \geq 2m$, while the armchair edge shows all the levels where $n \geq m \geq 1$. (iii) The states are much less dense than at the bottom of the band and Eq. (2) describes only the lowest states accurately. (iv) Due to the sparseness of the states, no supershell oscillations are visible for the massless particles (although the supershell structure of ordinary electrons is clearly seen in Fig. 2). (v) The zigzag edge supports particularly visible edge states^{27,28} that appear at ϵ_F as a prominent peak. The number of these states equals the number of the outermost edge atoms in zigzag triangles, which is $N_{ss} = \sqrt{N}$.

In order to compare our results to a more realistic calculation, we have performed DFT calculations for triangular $C_{321}H_{51}$ (zigzag) and $C_{330}H_{60}$ (armchair) flakes with the CPMD program.²⁹ The DFT calculations use a plane wave basis set ($E_{cut} = 50$ Ry), pseudopotentials,³⁰ and a generalized gradient-corrected Perdew–Burke–Ernzerhof approximation for the exchange–correlation energy.³¹ The resulting DFT-DOS of *all* valence electrons is plotted in Fig. 3(b) for both systems, and they show overall features characteristic

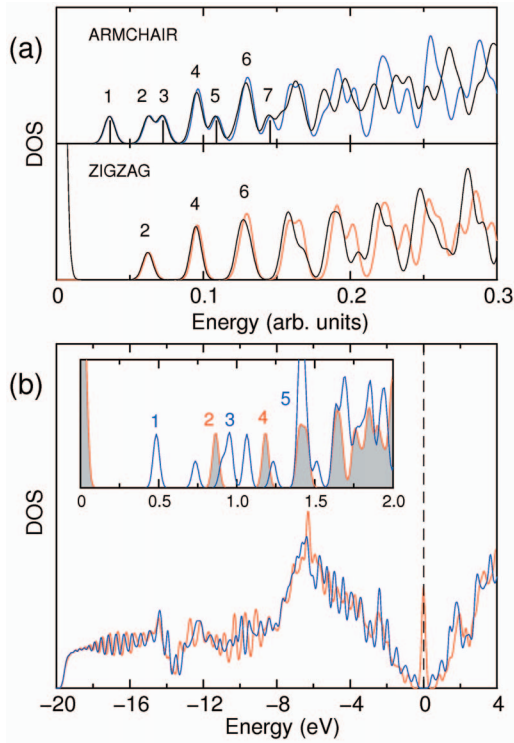


FIG. 3. (Color) Upper panel: TB-DOS at the Fermi level displayed as a function of energy (red and blue curves) compared to the density of levels of Eq. (2) (black curves). The zigzag triangle has 10 000 atoms and the armchair triangle 9918 atoms. Lower panel: DOS of the full DFT calculation for the triangular $C_{321}H_{51}$ (zigzag, red) and $C_{330}H_{60}$ (armchair, blue) flakes. The inset shows the levels above the Fermi surface where the zigzag spectrum is shaded.

for graphite. The zigzag edge states at ϵ_F are visible and the closest conduction states obey the simple analytical model of Eq. (2). The even-numbered peaks are split for the armchair triangle, which is a result reproduced by TB (the splitting reduces with increasing system size).

The lowest conduction states that are labeled in Fig. 3 show fascinating details and the electron densities of two such states are visualized in Fig. 4. For comparison, we show the same states and/or orbitals calculated for a large triangle with the TB model (4920 C atoms) and for a small triangle calculated with the DFT method (330 C atoms). The internal structure (symmetry) of the states is clearly similar, and therefore, it is independent of the triangle size and the model used. The states close to the Fermi level appear very different from those at the bottom of the band (Fig. 2). They are *not* simple densities of massless particles confined in a triangle since the density profile does not decay to zero at the edges. The corresponding electron levels are close to the Brillouin zone boundary, having large k values and the wave functions have pronounced oscillations with wavelengths that are related to the unit cell size. These oscillations guarantee that the wave function will be formally zero at the edges but the corresponding pseudowave function of the massless particle does not necessarily show the same behavior. An interesting feature in Fig. 4 is that the states have simple geometric structure of triangular symmetry. The size (number) of the

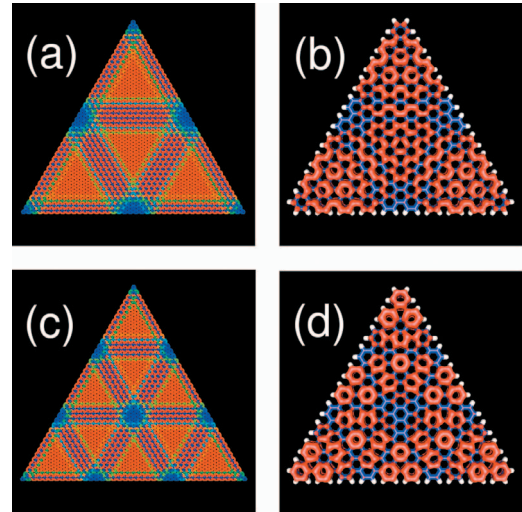


FIG. 4. (Color) Electron density of the [(a) and (b)] third and [(c) and (d)] fifth energy levels above the Fermi energy in armchair triangles (ghost states, labeled in Fig. 3, each has a degeneracy two). (a) and (c) are computed for a large TB triangle of 4920 C atoms, while (b) and (d) are DFT results for a $C_{330}H_{60}$ molecule.

triangles decreases (increases) with increasing energy, i.e., the pattern repeats itself. These “ghost states” are completely absent for the zigzag triangles, and they correspond to quantum numbers of Eq. (2) that are not allowed for free electrons in a triangular box [i.e., $2m \geq n \geq m \geq 1$ in Eq. (2)].

Figure 5 shows the electron densities corresponding to the “normal” low energy states that obey the standard selection rules ($m \geq 1$ and $n \geq 2m$). Again, the electron density does not necessarily vanish at the edges of the triangle. The corresponding states for the armchair and zigzag triangles display obvious differences despite the fact that they involve the same set of quantum numbers (and energy).

Finally, we want to note that a small roughness of the

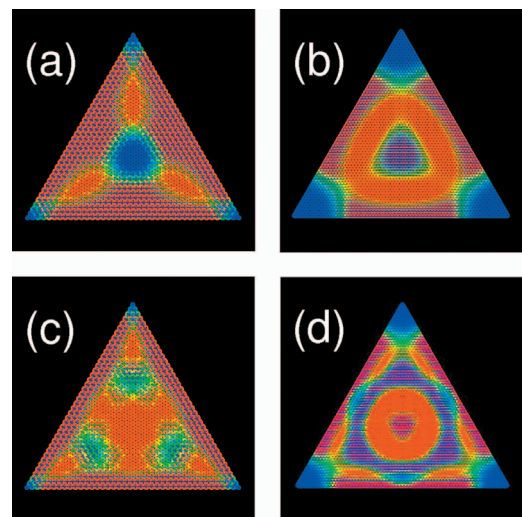


FIG. 5. (Color) Electron density (TB model) of the [(a) and (b)] second and [(c) and (d)] fourth energy levels above the Fermi energy (labeled in Fig. 3) for armchair and zigzag triangles of 4920 and 5181 C atoms, respectively.

edge does not remove the peculiar states shown in Fig. 4 or change the shell structure close to the Fermi level. These ghost states form a triangular network, and it would be interesting to study if they can exist also in the graphene flakes with hexagonal, parallelogram, or trapezoidal shapes.

In conclusion, we have computed the electronic structure of triangular graphene flakes and shown that the DOS profile close to ϵ_F is independent of the triangle size, and it can be described with the simple TB model. The zigzag flakes exhibit well-known edge states and the armchair triangles show an additional set of ghost states (different selection rules) where the corresponding electron density makes a triangular

pattern. In large triangles of 5000–10 000 C atoms, the energy levels can be accurately described by considering free massless particles confined in a triangular cavity. Presumably, the electronic states near the Fermi surface are not sensitive to the dielectric substrate, and we expect that these fascinating wave functions can be observed with scanning tunneling microscopy.

This work has been supported by the Academy of Finland. The DFT calculations were performed on IBM-SP4+ platforms at the John von Neumann Institute for Computing (NIC), Forschungszentrum Jülich, Germany.

-
- ¹C. Berger, Z. M. Song, T. B. Li, X. B. Li, A. Y. Ogbazghi, R. Feng, Z. T. Dai, A. N. Marchenkov, E. H. Conrad, P. N. First, and W. A. de Heer, *J. Phys. Chem.* **108**, 19912 (2004).
- ²K. S. Novoselov, A. K. Geim, S. V. Morozov, D. Jiang, Y. Zhang, S. V. Dubonos, I. V. Grigorieva, and A. A. Firsov, *Science* **306**, 666 (2004).
- ³K. S. Novoselov, A. K. Geim, S. V. Morozov, D. Jiang, M. I. Katsnelson, I. V. Grigorieva, S. V. Dubonos, and A. A. Firsov, *Nature (London)* **438**, 197 (2005).
- ⁴C. Berger, Z. M. Song, X. B. Li, X. S. Wu, N. Brown, C. Naud, D. Mayo, T. B. Li, J. Hass, A. N. Marchenkov, E. H. Conrad, P. N. First, and W. A. de Heer, *Science* **312**, 1191 (2006).
- ⁵J. Alicea and M. P. A. Fisher, *Phys. Rev. B* **74**, 075422 (2006).
- ⁶V. P. Gusynin and S. G. Sharapov, *Phys. Rev. Lett.* **95**, 146801 (2005).
- ⁷V. P. Gusynin, S. G. Sharapov, and J. P. Carbotte, *Phys. Rev. Lett.* **96**, 256802 (2006).
- ⁸K. Nomura and A. H. MacDonald, *Phys. Rev. Lett.* **98**, 076602 (2007).
- ⁹Y.-W. Son, M. L. Cohen, and S. G. Louie, *Phys. Rev. Lett.* **97**, 216803 (2006).
- ¹⁰K. S. Novoselov, Z. Jiang, Y. Zhang, S. V. Morozov, H. L. Stormer, U. Zeitler, J. C. Maan, G. S. Boebinger, P. Kim, and A. K. Geim, *Science* **315**, 1379 (2007).
- ¹¹A. K. Geim and K. S. Novoselov, *Nat. Mater.* **6**, 183 (2007).
- ¹²G. Li and E. A. Andrei, *Nat. Phys.* **3**, 623 (2007).
- ¹³S. Y. Zhou, G. H. Gweon, J. Graf, A. V. Fedorov, C. D. Spataru, R. D. Diehl, Y. Kopelevich, D.-H. Lee, S. G. Louie, and A. Lanzara, *Nat. Phys.* **2**, 595 (2006).
- ¹⁴M. Brack, J. Blaschke, S. C. Greagh, A. G. Magner, P. Meier, and S. M. Reimann, *Z. Phys. D: At., Mol. Clusters* **40**, 276 (1997).
- ¹⁵J. Kolehmainen, H. Häkkinen, and M. Manninen, *Z. Phys. D: At., Mol. Clusters* **40**, 306 (1997).
- ¹⁶E. Janssens, H. Tanaka, S. Neukermans, R. E. Silverans, and P. Lievens, *New J. Phys.* **5**, 46 (2003).
- ¹⁷S. M. Reimann, M. Koskinen, J. Helgesson, P. E. Lindelof, and M. Manninen, *Phys. Rev. B* **58**, 8111 (1998).
- ¹⁸M. Y. Lai and Y. L. Wang, *Phys. Rev. Lett.* **81**, 164 (1998).
- ¹⁹T. Yamamoto, T. Noguchi, and K. Watanabe, *Phys. Rev. B* **74**, 121409(R) (2006).
- ²⁰S. R. Elliot, *The Physics and Chemistry of Solids* (Wiley, New York, 1998).
- ²¹D. A. Areshkin, D. Gunlycke, and C. T. White, *Nano Lett.* **7**, 204 (2007).
- ²²M. Manninen, J. Mansikka-aho, and E. Hammarén, *Europhys. Lett.* **15**, 423 (1991).
- ²³F. E. Borghis and C. H. Papas, in *Encyclopedia of Physics*, edited by S. Flückie (Springer, Berlin, 1957).
- ²⁴H. R. Krishnamurthy, H. S. Mani, and H. C. Verma, *J. Phys. A* **15**, 2131 (1982).
- ²⁵S. M. Reimann, M. Koskinen, H. Häkkinen, P. E. Lindelof, and M. Manninen, *Phys. Rev. B* **56**, 12147 (1997).
- ²⁶Y.-Z. Huang, W.-H. Guo, L.-J. Yu, and H.-B. Lei, *IEEE J. Quantum Electron.* **37**, 1259 (2001).
- ²⁷K. Kobayashi, *Phys. Rev. B* **48**, 1757 (1993).
- ²⁸K. Nakada, M. Fujita, G. Dresselhaus, and M. S. Dresselhaus, *Phys. Rev. B* **54**, 17954 (1996).
- ²⁹CPMD Version 3, 11 Copyright IBM Corp., 1990–2006, Copyright MPI für Festkörperforschung Stuttgart 1997–2001 (www.cpmid.org).
- ³⁰N. Troullier and J. L. Martins, *Phys. Rev. B* **43**, 1993 (1991).
- ³¹J. P. Perdew, K. Burke, and M. Ernzerhof, *Phys. Rev. Lett.* **77**, 3865 (1996).